Multiple Roles of ADP-Ribosylation Factor 1 in Plant Cells Include Spatially Regulated Recruitment of Coatomer and Elements of the Golgi Matrix[1][W][OA]

Loren A. Matheson, Sally L. Hanton, Marika Rossi, Maita Latijnhouwers, Giovanni Stefano, Luciana Renna, and Federica Brandizzi*

Department of Biology, University of Saskatchewan, Saskatoon, Saskatchewan S7N 5E2, Canada (L.A.M., S.L.H., M.R., G.S., L.R., F.B.); Plant Pathology Program, Scottish Crop Research Institute, Invergowrie, Dundee DD2 5DA, United Kingdom (M.L.); and Department of Energy, Plant Research Laboratory, Michigan State University, East Lansing, Michigan 48824 (M.R., F.B.)

Recent evidence indicates that ADP-ribosylation factor 1 (ARF1) carries out multiple roles in plant cells that may be independent from the established effector complex COPI. To investigate potential COPI-independent functions, we have followed the dynamics of ARF1 and a novel putative effector, the plant golgin GRIP-related ARF-binding domain-containing Arabidopsis (*Arabidopsis thaliana*) protein 1 (GDAP1) in living plant cells. We present data that ascribe a new role to ARF1 in plant cell membrane traffic by showing that the GTPase functions to recruit GDAP1 to membranes. In addition, although ARF1 appears to be central to the recruitment of both COPI components and the golgin, we have established a different subcellular distribution of these ARF1 effectors. Live cell imaging demonstrates that GDAP1 and COPI are distributed on Golgi membranes. However, GDAP1 is also found on ARF1-labeled structures that lack coatomer, suggesting that the membrane environment, rather than ARF1 alone, influences the differential recruitment of ARF1 effectors. In support of this hypothesis, fluorescence recovery after photobleaching analyses demonstrated that GDAP1 and COPI have different kinetics on membranes during the cycle of activation and inactivation of ARF1. Therefore, our data support a model where modulation of the cellular functions of ARF1 in plant cells encompasses not only the intrinsic activities of the effectors, but also differential recruitment onto membranes that is spatially regulated.

Efficient membrane trafficking events require the activity of small GTPase ADP-ribosylation factors (ARFs; Memon, 2004). In animal and yeast cells, a single form of ARF-GTPase can have multiple activities that are crucial to the operation of the secretory pathway. A prime example of this complexity is provided by ARF1. In mammalian cells, ARF1 is involved in the regulation of COPI-mediated vesicular traffic of proteins from the Golgi to the endoplasmic reticulum (ER), as well as activation of lipid-modifying enzymes and recruitment of tethering/scaffolding molecules, such as Golgi matrix proteins (Donaldson et al., 2005).

In plant cells, the roles of ARF1 are less characterized compared to other eukaryotic systems. It has been suggested that ARF1 is involved in retrograde protein transport from the Golgi to the ER by interaction with COPI vesicle coat protein components (Movafeghi et al., 1999; Contreras et al., 2000; Pimpl et al., 2000; Takeuchi et al., 2002; Couchy et al., 2003). It has also been shown in plants that ARF1 mutants impaired in the GDP/GTP exchange can cause collapse of Golgi membranes into the ER, inhibition of ER export of soluble markers, and the loss of integrity of the ER export sites (Ritzenthaler et al., 2002; Takeuchi et al., 2002; daSilva et al., 2004; Stefano et al., 2006a). These observations indicated that ARF1 not only functions in retrograde protein transport to the ER but also indirectly affects the anterograde pathway (Brandizzi et al., 2002; Nebenführ et al., 2002; daSilva et al., 2004; Stefano et al., 2006a). In addition, plant ARF1 has been suggested to play a role in regulating protein transport to the vacuole, because a GTP-locked form of ARF1 induces secretion of vacuolar proteins and also inhibits constitutive secretion (Pimpl et al., 2003). Although the mechanisms for this function of ARF1 have not yet been fully elucidated, it has been shown that the GTPase is localized not only at the Golgi apparatus but also at additional structures of unknown nature that can bud from the Golgi (Xu and Scheres, 2005; Stefano et al., 2006a). Whether these ARF1-labeled structures are involved in protein transport to the vacuole or possess other functions is not yet known.

[1] This work was supported by Canada Foundation for Innovation, Canada Research Chair, Natural Sciences and Engineering Research Council of Canada, and Department of Energy (Michigan State University) grants to F.B.

* Corresponding author; e-mail brandizz@msu.edu; fax 517–353–9168.

The author responsible for distribution of materials integral to the findings presented in this article in accordance with the policy described in the Instructions for Authors (www.plantphysiol.org) is: Federica Brandizzi (brandizz@msu.edu).

[W] The online version of this article contains Web-only data.

[OA] Open Access articles can be viewed online without a subscription.

www.plantphysiol.org/cgi/doi/10.1104/pp.106.094953

Studies in nonplant systems have indicated that ARF1 is involved in the recruitment of a putative matrix protein GMAP210 (also known as CEV13/TRIP11/TRIP230 in mammalian cells and Rud3 in yeast) to the Golgi apparatus (Gillingham et al., 2004). The interaction of GMAP210 and homolog proteins with ARF1 occurs through a conserved COOH-terminal GRIP-related ARF-binding domain (Gillingham et al., 2004). The conservation of the positions of certain amino acid residues in the sequence of this domain has allowed the identification of an Arabidopsis (*Arabidopsis thaliana*) homolog to GMAP210 (Latijnhouwers et al., 2005). Whether ARF1 is involved in the recruitment of the homolog golgin to Golgi membranes in plants cells as well is unknown.

The evidence that ARF1 has multiple cellular roles raises the important question of how the specificity of ARF1-mediated processes is acquired. It is possible that the specificity is solely restricted to the activity of downstream ARF1 effectors, such as COPI and tethering/scaffolding factors. However, the possibility also exists that the interaction of various ARF1-regulating factors that are found only on specific organelles may serve to spatially and temporally coordinate the activity of the GTPase. Plant ARF1 is an ideal element by which to address these hypotheses, as it is localized not only on the Golgi apparatus with coatomer (Pimpl et al., 2000; Ritzenthaler et al., 2002) but also on additional structures that lack coatomer (Xu and Scheres, 2005; Stefano et al., 2006a). The biological role of ARF1 on these structures is unknown, but it most likely involves specific effectors. Therefore, we sought to use the plant system to gain further insights on the role of this important GTPase in plants and to investigate the regulation of ARF1 activation in conjunction with the kinetics of various ARF1 effectors on membranes.

Our findings ascribe a novel role to plant ARF1, as the GTPase was found to interact directly with the plant homolog of GMAP210. This protein was recruited directly by ARF1 on the Golgi apparatus and on the additional non-Golgi ARF1 structures that lack coatomer. These data suggest that the composition of the target membranes is key to the specification of effector recruitment mediated by ARF1. We analyzed the process of association and dissociation of COPI and the golgin on and off membranes and related it to the dynamics of ARF1. The kinetics of the golgin, but not of COPI, were strictly dependent on the cycles of activation and inactivation of ARF1 on the membranes. Because the kinetics of ARF1 differ in comparison to that of its effectors, the specificity of ARF1 relies on the nature of the effectors and their membrane environment rather than on the intrinsic properties of ARF1.

RESULTS

ARF1 Is Distributed in the Same Cellular Compartments as GDAP1, a Golgi Matrix Protein

The Arabidopsis genome encodes a sequence with 32% identity and 62% similarity at the amino acid level to the human GMAP210 (Latijnhouwers et al., 2005) that we propose be called GRIP-related ARF-binding domain-containing Arabidopsis protein 1 (GDAP1). GDAP1 is a protein of 712 amino acid residues with a predicted molecular mass of 81.7 kD.

To determine the subcellular localization of GDAP1, we fused it to a yellow fluorescent protein (YFP-GDAP1) and expressed it in tobacco (*Nicotiana tabacum*) leaf epidermal cells. Laser confocal microscopy analyses indicated that YFP-GDAP1 labeled punctate structures of heterogeneous size (≤ 1 μm in diameter) that were motile in the cell (Fig. 1A). The larger structures labeled by YFP-GDAP1 were often observed in a distinct ring formation (Fig. 1B).

As the punctate subcellular distribution of YFP-GDAP1 resembled that of the plant Golgi apparatus, tobacco leaf epidermal cells were cotransformed with the YFP-GDAP1 fusion and the ER/Golgi marker ERD2-GFP (Boevink et al., 1998). ERD2-GFP colocalized with the larger punctate structures of YFP-GDAP1. However, other structures were labeled solely by YFP-GDAP1 (Fig. 1, C–E).

The distribution of GDAP1 was similar to that of ARF1, which mainly localizes to the Golgi apparatus but also additional non-Golgi structures (Xu and Scheres, 2005; Stefano et al., 2006a). To test this further, we coexpressed YFP-GDAP1 with ARF1-GFP (Stefano et al., 2006a). All the structures labeled by YFP-GDAP1 showed colocalization with ARF1-GFP (Fig. 1, F–H). This shows that the GTPase and GDAP1 colocalize to extra-Golgi structures. Furthermore, ARF1-GFP structures were stained by the styryl dye FM4-64, which labels compartments localized to the endocytic route (Bolte et al., 2004; Supplemental Fig. S1), consistent with earlier findings (Xu and Scheres, 2005).

Binding of GDAP1 to Membranes Depends on ARF1 Activity

The colocalization results of ARF1 and GDAP1 led us to question whether GDAP1 could be functionally linked to ARF1. To explore this, we wanted to test the influence of ARF1 on GDAP1 recruitment to membranes. ARF1 directly recruits coatomer to membranes in its active form (Serafini et al., 1991; Donaldson et al., 1992; Memon, 2004). We postulated that, if similarly to coatomer, ARF1 recruits GDAP1 to membranes, expression of the GTP-restricted mutant of $ARF1^{Q71L}$, which mimics the active form of ARF1 (Teal et al., 1994; Pimpl et al., 2000), would enhance signal of the golgin on membranes in comparison to a control expressing GDAP1 alone. To test this hypothesis, we coexpressed YFP-GDAP1 with $ARF1^{Q71L}$, which is known to overlap with the distribution of wild-type ARF1 (Fig. 2A; Stefano et al., 2006a). We assessed GDAP1 recruitment by taking measurements of the fluorescence intensity within areas of identical size that included the punctate structures labeled by YFP-GDAP1 alone or in combination with $ARF1^{Q71L}$ normalized to the fluorescence intensity of the corresponding cytosolic fraction of

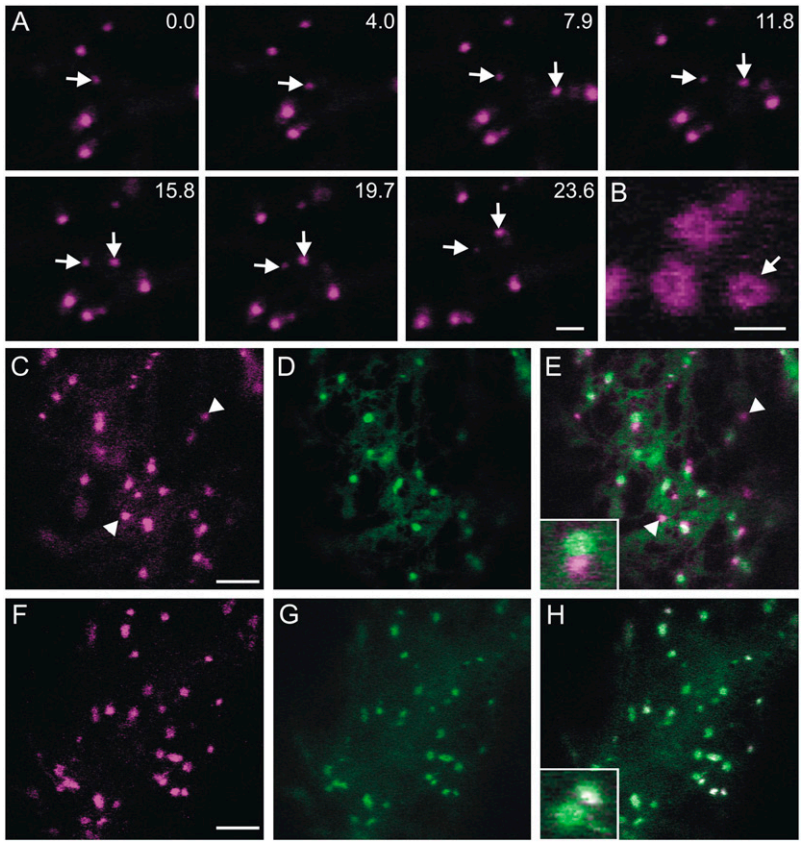

Figure 1. The subcellular distribution of GDAP1 overlaps that of ARF1. A, Images from a time-lapse sequence of confocal images of tobacco leaf epidermal cells expressing YFP-GDAP1. Time(s) of frame acquisition is indicated at the top right corner. The arrows indicate motile structures labeled by YFP-GDAP1. Scale bar = 5 μm. B, High magnification image of YFP-GDAP1 demonstrating large ring structures. Scale bar = 2 μm. C, Confocal images of YFP-GDAP1 coexpressed with the ER/Golgi marker ERD2-GFP. GDAP1 is localized at Golgi bodies and at additional structures (arrowhead; inset in E, merged image of C and D). YFP-GDAP1 (F) colocalized with all structures labeled by ARF1-GFP (G). H, Merged image of F and G. Inset shows detail of H. Scale bars in C and F = 5 μm.

each coat component (see also ''Materials and Methods''). With the same approach, we quantified the recruitment of COPI on membranes in the presence of ARF1^{Q71L} using a fluorescent fusion of the component εCOP-YFP (Fig. 2C; Stefano et al., 2006a).

As shown in Figure 2, B and D, the values of relative fluorescence intensity of punctate structures in cells coexpressing the GTPase with either YFP-GDAP1 or εCOPI-YFP were significantly higher than those gathered in the respective control cells ($P < 0.05$; $n = 75$ in 45 cells or $n = 65$ in 30 cells, respectively). These data provide evidence that ARF1 is involved in the recruitment of GDAP1 to membranes as it does for COPI.

To confirm that the distribution of GDAP1 on membranes was dependent on ARF1 activation, leaf epidermal cells coexpressing YFP-GDAP1 and ARF1-GFP were treated with brefeldin A (BFA), which is known to interfere with ARF1 activation (Robineau et al., 2000). We then followed the distribution of YFP-GDAP1 and ARF1-GFP over time. If active ARF1 is involved in the membrane recruitment of YFP-GDAP1, inactivation of ARF1 would lead to redistribution of GDAP1 into the cytosol. A time course showed that both GDAP1 and ARF1 were released into the cytosol at the same time upon treatment of cells with the inhibitor (Fig. 3, A and B). This effect did not occur in the control samples without BFA, indicating that our data were not the result of photobleaching during the course of the experiment (Fig. 3C; Supplemental Fig. S2). These data imply that the inactivation of ARF1 is associated with the release of GDAP1 from membranes.

The Interaction of ARF1 with GDAP1 Is Direct

Although the data presented above indicate that ARF1 is involved in the distribution of GDAP1 on the membranes where ARF1 resides, they do not distinguish whether the interaction of ARF1 and GDAP1 is direct or mediated by other factors. To test this, we developed a glutathione-agarose affinity chromatography assay based on the interaction of a recombinant glutathione *S*-transferase (GST)-GDAP1 with recombinant ARF protein. We used extracts of *Escherichia coli* expressing His_6 fusions of ARF1wt, ARF1^{Q71L}, and ARF1^{T31N}, the GDP-locked mutant, and loaded them on glutathione columns that had been preloaded with extracts of *E. coli* expressing GST-GDAP1. Eluates of the columns were subjected to immunoblot analysis with either anti-His_6 or anti-GST serum (Fig. 4A). The chemiluminescence signal was acquired on the same membrane with a short exposure (20 s) and long exposure (60 s) to allow comparison of the signals without oversaturating pixels and compromising a clear detection of weak signals. Results indicate that there is an interaction between GDAP1 and ARF1wt, ARF1^{Q71L}, and ARF1^{T31N}; however, there was preferential association of GDAP1 with the wild type and GTP-locked ARF1 (Fig. 4A, lanes 5–7 and 13–15).

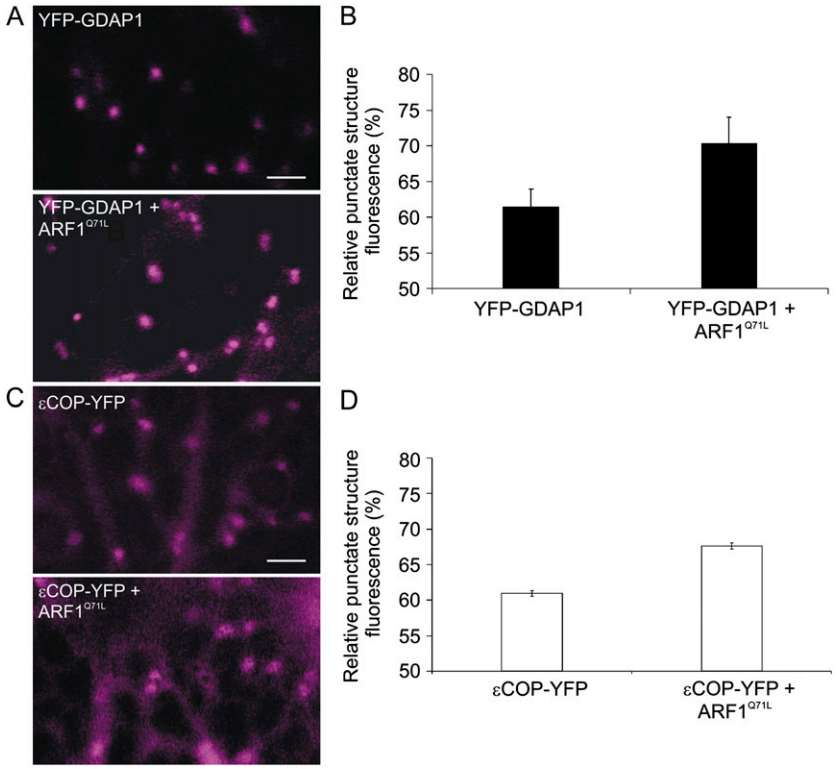

Figure 2. Coexpression of active ARF1 and GDAP1 enhances the recruitment of the golgin onto the Golgi apparatus. A, Confocal images of the YFP channel only of cells expressing either YFP-GDAP1 alone or YFP-GDAP1 with untagged ARF1^{Q71L}, which mimics the active form of ARF1 (Teal et al., 1994; Pimpl et al., 2000). The presence of untagged ARF1 in cells was ensured by using a double cistronic vector encoding ARF1^{Q71L} and the peroxisomal marker, CFP-SKL (Stefano et al., 2006a). Fluorescence quantification was carried out in cells where both the YFP and CFP signals were present. Scale bar = 5 μm. B, The fluorescence of the punctate structures relative to that of the cytosol was quantified for YFP-GDAP1 alone or coexpressed with ARF1^{Q71L}. The RPSF is given as a percentage of the ratio between fluorescence intensity values (arbitrary units) measured in the cytosol and the sum of intensity values for the cytosol and punctate structures (see "Materials and Methods"). We found that the intensity of punctate structure fluorescence increased significantly when YFP-GDAP1 was coexpressed with ARF1^{Q71L} ($P < 0.05$). Error bars represent SDs for 75 measurements over 45 different cells. C, Confocal images of cells expressing either εCOP-YFP alone or with untagged ARF1^{Q71L} (YFP channel only) encoded in an ARF1^{Q71L}-CFPSKL double cistronic vector, as described in A and B, above. D, Quantification of the RPSF fluorescence shows that in the presence of ARF1^{Q71L}, the signal of εCOP-YFP increases on the Golgi membranes ($P < 0.05$). Error bars represent SDs for 65 measurements over 30 different cells.

Expression of the ARF proteins was tested by western blot on a fraction of total *E. coli* extracts to verify that similar quantities of ARF1 wild type, GTP, and GDP were loaded on the GST-GDAP1 columns (Fig. 4A, lanes 1–3).

As the GTPase cycle of the wild-type ARF1 prevents us from knowing whether ARF1wt in Figure 4A was in the active or inactive form, we decided to use non-hydrolyzable analogs of GTP and GDP, thus ensuring that the results were independent of the mutations. Wild-type ARF1 was charged with either GTPγS or GDPβS, and the interaction with GST-GDAP1 was tested (Fig. 4B). ARF1-His$_6$ was retained by immobilized GST-GDAP1 with and without exogenous GTP and GDP (Fig. 4B, lanes 5–7 and 13–15). Similar to Figure 4B, the GDP-loaded ARF1-His$_6$ had a decreased affinity for the GST-GDAP1.

The column loaded with GST alone did not retain any ARF1 protein in either experiment under either exposure length (Fig. 4, A and B, lanes 9–12, 17–20). Anti-GST immunoblots demonstrated that GST-GDAP1 (Fig. 4, A and B, lanes 21–24) or GST (Fig. 4, A and B, lanes 25–28) were present in the column in comparable quantities.

These data demonstrate that the association of ARF1 with GDAP1 occurs preferentially with active ARF1, therefore supporting our microscopy data on the recruitment and release of GDAP1 from membranes in the presence of either active or inactive ARF1, respectively (Figs. 2 and 3). They also prove that the interaction of GDAP1 with ARF1 is due to a direct association of the two molecules.

The Kinetics of GDAP1 on Membranes Are ARF1 Dependent

The membrane dissociation of YFP-GDAP1 induced by BFA (Fig. 3) suggests that the association of GDAP1

on membranes is not stable. Therefore, to characterize further the kinetics of GDAP1 on membranes, we performed fluorescence recovery after photobleaching (FRAP) experiments on the punctate structures labeled by YFP-GDAP1. Photobleaching of YFP-GDAP1 was followed by a rapid recovery of YFP fluorescence on the membranes (Fig. 5, A and B), confirming that GDAP1 does not associate stably with membranes.

To substantiate that the kinetics of the golgin on membranes are dependent on ARF1, we performed FRAP experiments on membranes labeled with YFP-GDAP1 in cells expressing ARF1^{Q71L}. FRAP experiments were conducted with the assumption that to maintain steady-state fluorescence levels, there must be an equal, continual loss of protein from the bleached organelle if the chimeric protein levels on the organelle membrane had reached a steady state at the start of each experiment. Therefore, we hypothesized that if the cycling of GDAP1 on and off membranes is dependent on the cyclic activation/inactivation of ARF1, the presence of the active mutant form of ARF1 in cells expressing GDAP1 would reduce the dynamic exchange of the organelle-associated GDAP1 fraction with its cytosolic pool. Consistent with our hypothesis, we found that the cycling of the golgin was affected by the presence of the ARF1 mutant, as the recovery of YFP fluorescence was significantly reduced in cells coexpressing ARF1^{Q71L} (half time = 16.13 ± 0.91 s;

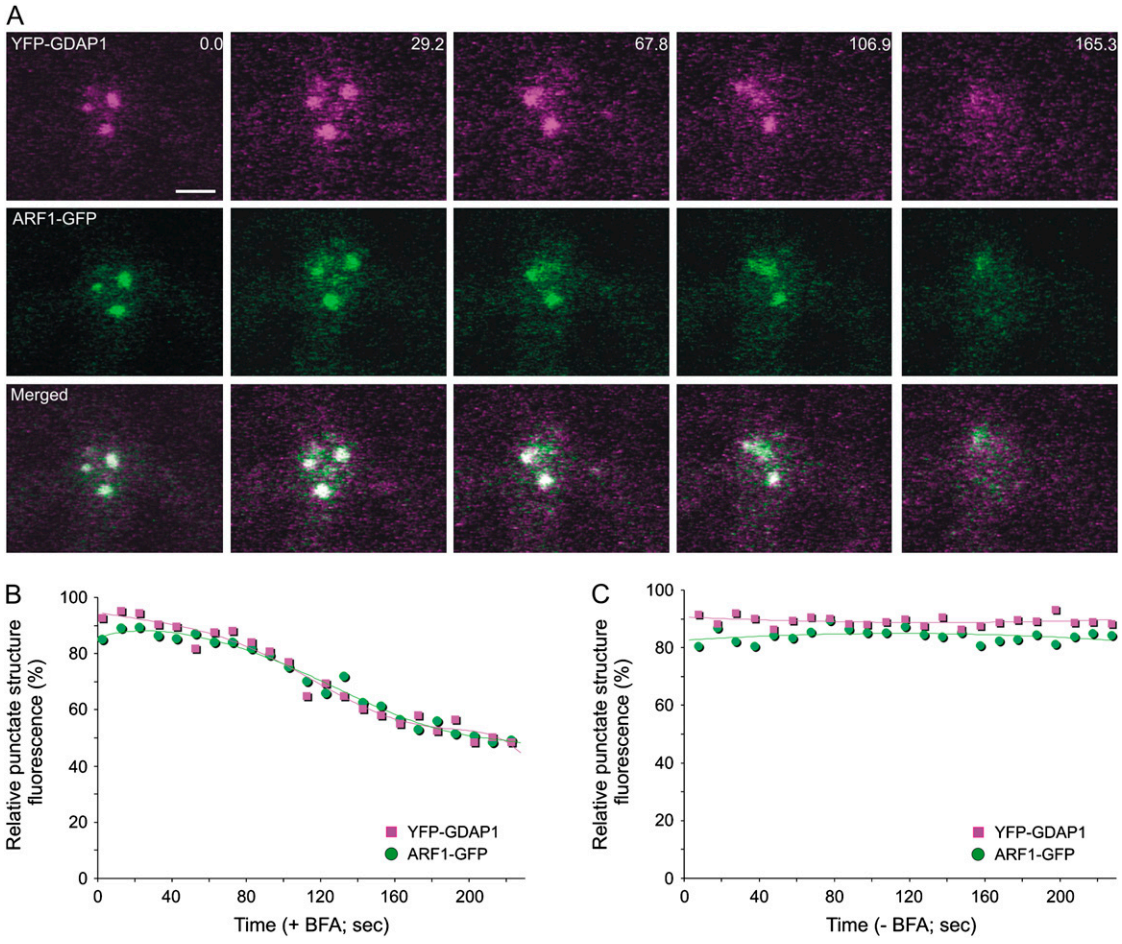

Figure 3. BFA treatment induces the simultaneous redistribution of YFP-GDAP1 and ARF1-GFP. A, Time-lapse confocal micrographs demonstrate the effect of BFA treatment on a live tobacco epidermal cell coexpressing YFP-GDAP1 and ARF1-GFP. The distribution of both markers was clearly visible on punctate structures before BFA treatment. Representative images are shown at various time points throughout the BFA treatment. There was variability observed in the response rate of ARF1-labeled structures within a given cell. In addition, temporal inconsistencies in response to BFA treatment were also observed between cells, in agreement with the observations of Ritzenthaler et al. (2002). However, the trend always remained consistent in that both ARF1 and GDAP1 were simultaneously released into the cytosol from the same structures. The time(s) is indicated in the top right corner. The first image in the sequence (labeled 0.0) was taken after a 45-min pretreatment with latrunculin B and a subsequent incubation of 5 min with BFA. Scale bar = 2 μm. The fluorescence of the punctate structures relative to that of the cytosol was measured for both YFP-GDAP1 and ARF1-GFP in each frame of the time lapse with (B) and without (C) BFA treatment. The RPSF is given as a percentage of the ratio between fluorescence intensity values (arbitrary units) measured in the punctate structure and the sum of intensity values for the cytosol and punctate structure (see "Materials and Methods").

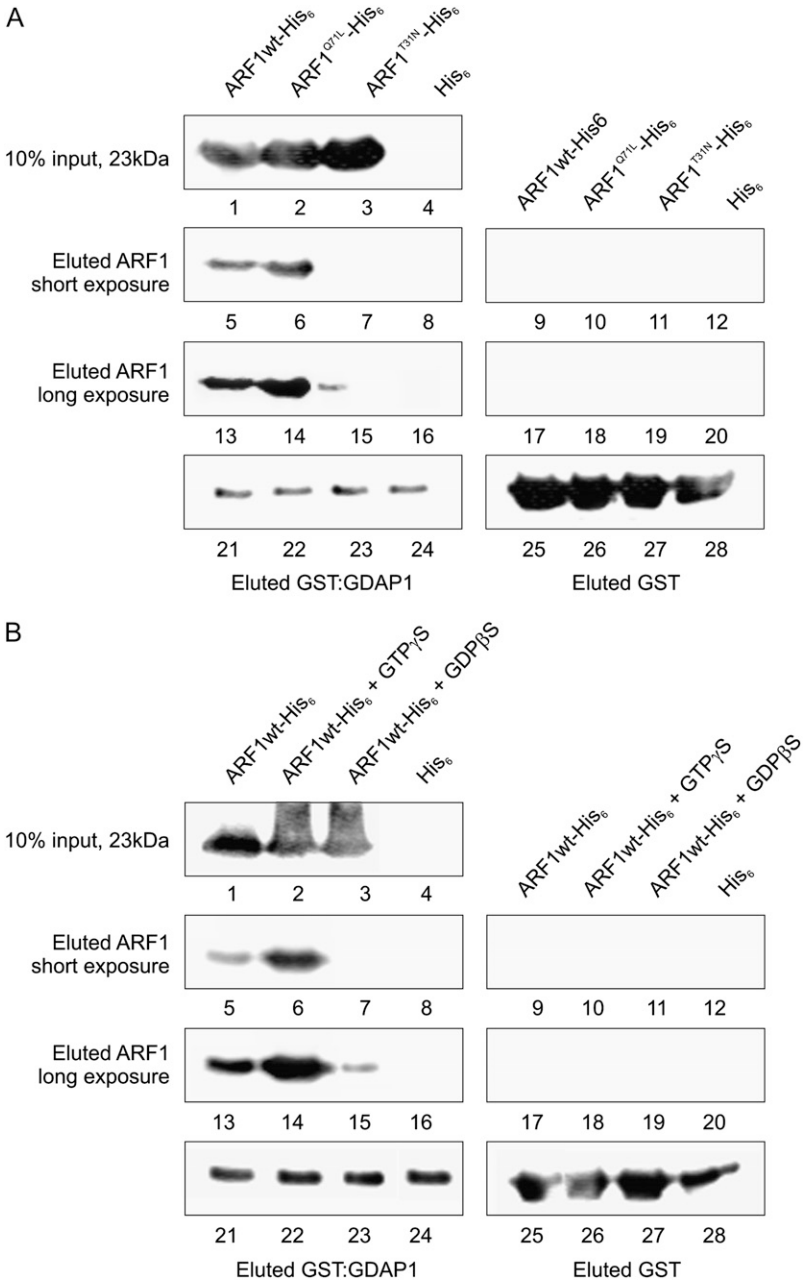

Figure 4. ARF1^{Q71L} is capable of a direct interaction with GDAP1. A, Interaction of recombinant His$_6$-tagged ARF1 wild type (ARF1wt) and mutants with GST-GDAP1 in vitro. Lanes 1 to 3, An immunoblot with a His$_6$ antibody on a 10% fraction of each *E. coli* extract was performed to test whether comparable amounts of ARF1wt-His$_6$ (lane 1), ARF1^{Q71L}-His$_6$ (lane 2), and ARF1^{T31N}-His$_6$ (lane 3) were loaded onto the columns. Lane 4, negative control, extract from *E. coli* expressing His$_6$-tag alone. Lanes 5 to 12, a short exposure of an immunoblot with anti-His$_6$ serum on column eluates demonstrates that there was retention of ARF1wt-His$_6$ (lane 5) as well as ARF1^{Q71L}-His$_6$ (lane 6) by GST-GDAP1. There was no detectable signal of ARF1^{T31N}-His$_6$ at this exposure length (lane 7). Negative controls, His$_6$ alone (lane 8). There was no retention of the His$_6$-tagged ARF proteins (lanes 9–11) or the His$_6$ tag alone (lane 12) by GST alone. Lanes 13 to 20, a longer exposure of the same membrane demonstrates that there is in fact a low affinity for ARF1^{T31N} by GDAP1 (lane 15). GST-GDAP1 preferentially retains ARF1wt-His$_6$ (lane 13) and ARF1^{Q71L}-His$_6$ (lane 14). The negative controls (lanes 16–20) were as described above for lanes 8 to 11. Lanes 21 to 24, immunoblot with anti-GST serum on column eluates demonstrates that GST-GDAP1 and GST were present on the columns in similar quantities. Therefore, any differences in the retention of ARF1 or its mutants were due to differences in the affinity of GDAP1 for the interaction. B, In vitro interaction of GST-GDAP1 with recombinant ARF1wt-His$_6$ charged with nucleotides. This experiment was performed and presented as in A, with the exception of using ARF1wt-His$_6$ coupled with either GTPγS or GDPβS in place of ARF1^{Q71L}-His$_6$ and ARF1^{T31N}-His$_6$, respectively. These results confirmed the observations (A) showing that ARF1 does interact with GDAP1 directly, and the inactive form of ARF1 has a decreased affinity for the golgin.

$n = 12$; Fig. 5, C and D) in comparison to the control (half time = 8.25 ± 0.25 s; $n = 15$, $P < 0.05$; Fig. 5, A and B). These data indicate not only that the activation of ARF1 is necessary for the binding of GDAP1 to membranes, but they also show that its dynamic cycle is dependent on the efficiency of GTP hydrolysis of ARF1.

The Effectors of ARF1 Have Different Kinetics on Membranes

It has been shown that ARF1 and coatomer cycle at different rates on and off membranes (Stefano et al., 2006a). The identification of GDAP1 as an effector of ARF1 prompted us to determine whether GDAP1 undergoes cycling on and off membranes with similar dynamics to COPI. FRAP experiments confirmed that both ARF1-GFP (half time = 7.71 ± 0.91 s; $n = 12$; Fig. 5, E and F) and its effector εCOP-YFP (half time = 19.85 ± 0.25, $n = 10$; Fig. 5, G and H) were found to cycle with different kinetics ($P < 0.05$), in accordance with previous findings (Stefano et al., 2006a). However, we found no significant difference between the rate of fluorescence recovery for ARF1-GFP (Fig. 5, E and F) and YFP-GDAP1 ($P < 0.05$; Fig. 5, A and B), indicating that these two proteins cycle with the same kinetics. In addition, both ARF1-GFP and YFP-GDAP1 labeling the extra-Golgi punctate structures cycle at the same

rate as the Golgi-localized ARF1 and GDAP1 (Fig. 5, A–F). However, the exchange of COPI on membranes was significantly slower than that of YFP-GDAP1 (Fig. 5, E and F; $P < 0.05$). These data indicate that although coatomer and GDAP1 are both recruited by ARF1 on membranes, the binding cycles of the two molecules are differentially regulated.

Inactivation of ARF1 Leads to a Temporal Difference in Effector Release from Golgi Membranes

Because εCOP-YFP and YFP-GDAP1 have different cycling half times, we postulated that inactivation of ARF1 could be one possible mechanism regulating the differential release of the effectors into the cytosol. To test this hypothesis, we first treated cells cotransformed with εCOP-YFP and ARF1-GFP with BFA. This allowed a comparison with the BFA treatment of cells coexpressing ARF1 and GDAP1 (Fig. 3). A time course following fluorescence intensity shows that upon the addition of BFA, εCOP-YFP is redistributed to the cytosol before ARF1-GFP (Fig. 6, A and B). This was interesting, as it was in clear contrast to what was observed in Figure 3, where ARF1-GFP and YFP-GDAP1 were released from membranes at the same time. As a control, a time course of images taken with the same settings on untreated cells transformed with

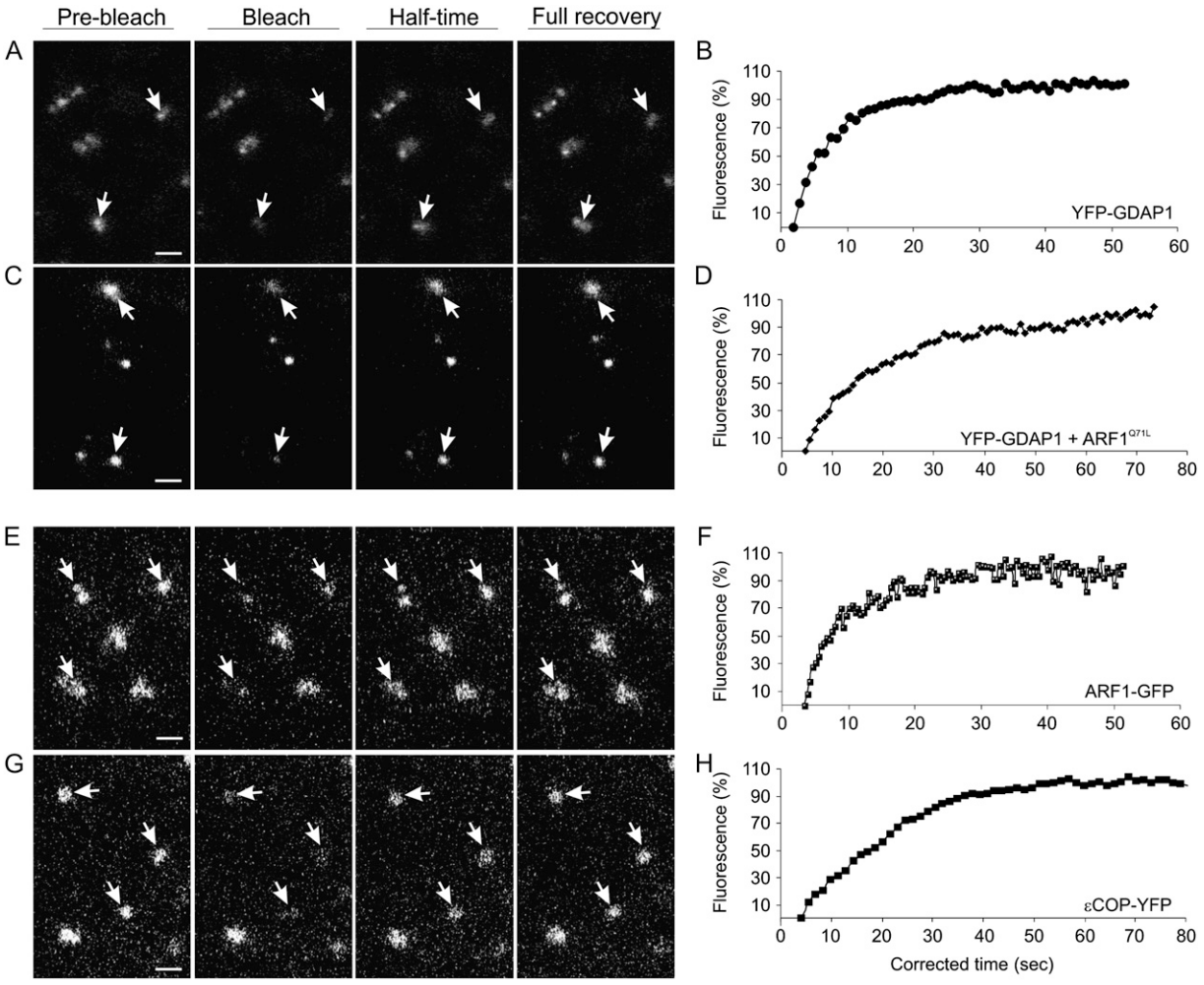

Figure 5. The membrane cycling kinetics of ARF1 effectors are different. Results of qualitative FRAP experiments on a cortical section of tobacco leaf epidermal cells expressing GDAP1-YFP (A), coexpressing YFP-GDAP1 and ARF1^{Q71L}-CFPSKL (C; Stefano et al., 2006a), ARF1-GFP (E), and εCOP-YFP (G). Samples were treated with latrunculin B to stop movement of Golgi and additional non-Golgi fluorescent structures. Each image in the horizontal sequence represents a prebleach, bleach, half-time recovery, or full recovery event, as indicated. Arrows indicate punctate structures that were bleached. Note that the smaller punctate structures of ARF1 recover with the same half time as Golgi-localized ARF1 (E). Scale bars = 2 μm. Half-time recovery curves of the fluorescence in cells expressing YFP-GDAP1 (B; 8.25 ± 0.25 s, $n = 15$), YFP-GDAP1 + ARF1^{Q71L}-CFPSKL (D; 16.13 ± 0.91 s, $n = 12$), ARF1-GFP (F; 7.71 ± 0.91 s, $n = 12$), and εCOP-YFP (H; 19.85 ± 0.25 s, $n = 10$) are also shown. Half time is defined as the time required for the fluorescence in the photobleached region to recover to 50% of the recovery asymptote, and n represents the number of bleached Golgi stacks.

both markers did not show significant reduction of fluorescence levels, therefore excluding the possibility that our results were due to photobleaching during the imaging process (Fig. 6C; Supplemental Fig. S3). Taken together, the results indicate that εCOP distribution on membranes was affected by the BFA treatment before GDAP1, suggesting that the interaction between ARF1 and its effectors is regulated at a level specific to the effector rather than the GTPase.

To confirm this, we treated cells cotransformed with εCOP-YFP and cyan fluorescent protein (CFP)-tagged GDAP1 with BFA. This allowed us to follow the release of both effectors from the same membranes simultaneously. A time course following fluorescence intensity shows that upon addition of BFA, coatomer fluorescence was quickly released from the Golgi membranes (Fig. 7, A and B). Although the Golgi-associated fluorescence of CFP-GDAP1 diminished over time, CFP-GDAP1 residual fluorescence was nonetheless still detectable on the Golgi after εCOP-YFP fluorescence was redistributed into the cytosol. Quantification of the fluorescence intensities of a time course of images taken from a control sample without BFA demonstrated that our results were not due to photobleaching (Fig. 7C; Supplemental Fig. S4). Our data are consistent with the findings that the release of GDAP1 from Golgi membranes occurs at the same time as the redistribution of ARF1 in the cytosol, but with different kinetics to coatomer (Figs. 3 and 6). This suggests that additional mechanisms are involved in the activity of ARF1-ligand interactions besides the direct recruitment of effectors by ARF1 on membranes.

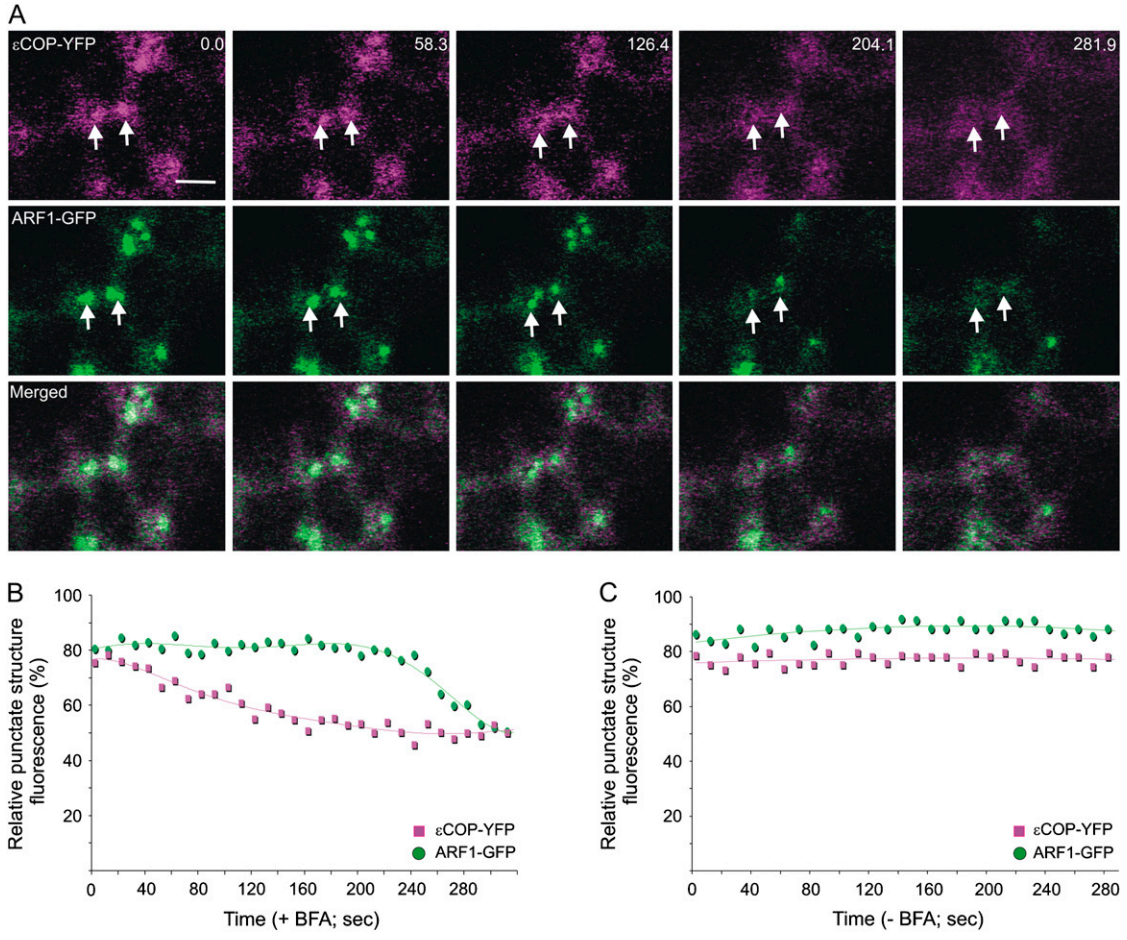

Figure 6. εCOP is more sensitive to BFA treatment than is ARF1. A, Time-lapse confocal micrographs demonstrate the effect of BFA treatment on a live tobacco epidermal cell coexpressing εCOP-YFP and ARF1-GFP. Representative images are shown with the time(s) indicated in the top right corner. The first image in the sequence (labeled 0.0) was taken after a 45-min pretreatment with latrunculin B and a subsequent incubation of 5 min with BFA. The images show that εCOP-YFP fluorescence is released from the Golgi (arrow) prior to the release of ARF1-GFP in the cytosol. Scale bar = 5 μm. The fluorescence of the punctate structures relative to that of the cytosol was measured for both ARF1-GFP and εCOP-YFP in each frame of the time lapse with (B) and without (C) BFA treatment. The RPSF is given as a percentage of the ratio between fluorescence intensity values (arbitrary units) measured in the punctate structure and the sum of intensity values for the cytosol and punctate structure (see "Materials and Methods").

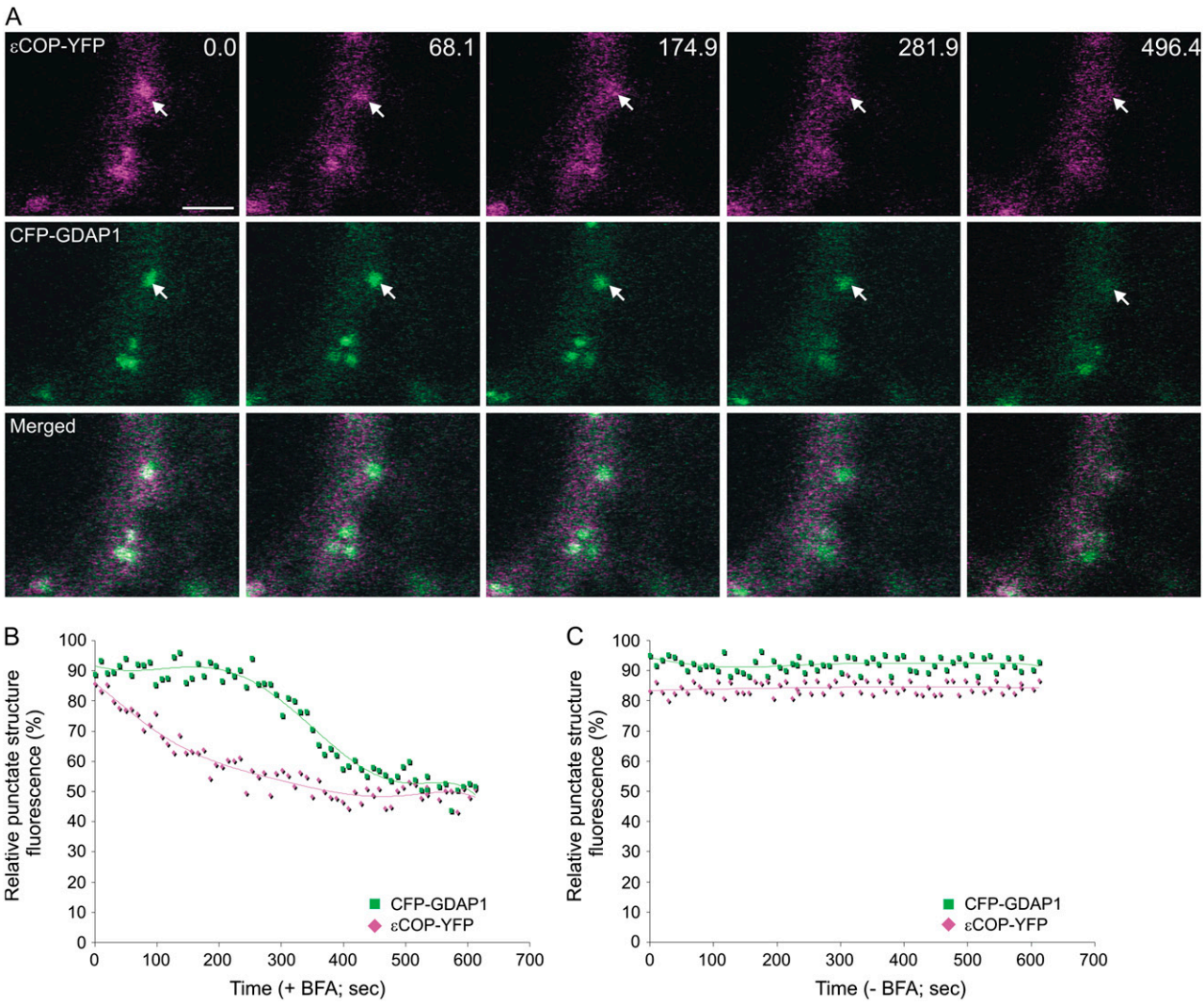

Figure 7. ARF1 effectors demonstrate different sensitivities to BFA. A, Time-lapse confocal micrographs demonstrate the effect of BFA treatment on a live tobacco epidermal cell coexpressing YFP-GDAP1 and εCOP-YFP. Representative images are shown with the time in seconds indicated in the top right corner. The first image in the sequence (labeled 0.0) was taken after a 45-min pretreatment with latrunculin B and a subsequent incubation of 3.5 min with BFA. The images indicate that εCOP-YFP fluorescence is released from the Golgi, whereas CFP-GDAP1 remains on punctate structures. Scale bar = 5 μm. The fluorescence of the Golgi relative to that of the cytosol was measured for both GDAP1-CFP and εCOP-YFP in each frame of the time lapse with (B) and without (C) BFA treatment. The RPSF is given as a percentage of the ratio between fluorescence intensity values (arbitrary units) measured in the punctate structure and the sum of intensity values for the cytosol and punctate structure (see "Materials and Methods").

DISCUSSION

GDAP1 Is a Novel Effector of ARF1 in Plant Cells

Our data show that the distribution of ARF1 and the putative golgin GDAP1 largely overlap in plant cells (Fig. 1). The evidence that ARF1 recruits GDAP1 to membranes in live cells (Fig. 2) via a direct interaction (Fig. 4), as it does with coatomer (Donaldson et al., 1992; Memon, 2004), strongly indicates that GDAP1 is a novel effector of ARF1 in plants. Although the cellular role of GDAP1 remains unknown, its codistribution with ARF1 suggests that ARF1 may participate in additional functions besides COPI recruitment on Golgi membranes. Plant ARF1 has been implicated in the vacuolar sorting route to the lytic vacuole (Pimpl et al., 2003) in addition to its well-known contribution to COPI vesicle formation (Pimpl et al., 2000; Couchy et al., 2003). More recent studies also demonstrated a role of the GTPase in apical-basal epidermal polarity during multicellular development (Xu and Scheres, 2005). In addition, the activation of ARF1 was shown to be of importance to maintain protein trafficking out of the ER (Stefano et al., 2006a) as well as being essential for endocytosis in plants (Xu and Scheres,

2005). The latter investigations have also reported a distribution of ARF1 not only on the Golgi apparatus but also on non-Golgi structures that we found to be targeted by GDAP1. This supports the hypotheses that ARF1 could have additional roles in which GDAP1 may be involved and that this function could be uncoupled from the ARF1-mediated recruitment of COPI on Golgi membranes.

The function of the ARF1- and GDAP1-labeled extra-Golgi punctate structures remains undetermined. Confocal time lapse imaging indicated that these structures can originate from the Golgi apparatus (Xu and Scheres, 2005; Stefano et al., 2006a) and may therefore be involved in post-Golgi trafficking. In support of the hypothesis suggesting an involvement of GDAP1 in post-Golgi traffic, studies have implicated ARF1 in processes distal to the classic COPI retrieval route (Stamnes and Rothman, 1993; Puertollano et al., 2001). Furthermore, the route between the trans-Golgi network and the vacuole was more sensitive to the GTP-locked mutant of ARF1 than was either COPI or COPII (Pimpl et al., 2003). Considering the close association of GDAP1 and ARF1 on post-Golgi compartments, there may be involvement of GDAP1 in the ARF1-mediated processes relevant to the vacuolar sorting route.

In addition, the localization of ARF1 on the non-Golgi structures labeled with FM4-64 (Xu and Scheres, 2005) suggests that GDAP1 may be involved in endocytic processes regulated by ARF1 in plant cells (Xu and Scheres, 2005). In protists, yeast, and animals, ARF1 has indeed been implicated in endocytosis (Zhang et al., 1994; Gaynor et al., 1998; Gu and Gruenberg, 2000; Yahara et al., 2001; Faure et al., 2004; Price et al., 2007). However, it is also possible that the non-Golgi structures labeled by ARF1 and GDAP1 may be endosomal compartments where the endocytic and secretory pathways meet, as has been recently suggested for the trans-Golgi network (Dettmer et al., 2006; Lam et al., 2007). This hypothesis would reconcile the evidence that the ARF1/GDAP1-labeled structures that bud from the Golgi apparatus (this work; Stefano et al., 2006a) are also labeled by endocytic markers (this work; Xu and Scheres, 2005).

In this study, we also show that GDAP1 is a component of the Golgi apparatus (Fig. 1). Although the function of GDAP1 within the plant Golgi apparatus is unknown, defects in glycosylation by yeast Golgi lacking Rud3, the yeast homolog of GDAP1, imply a role in retrograde traffic (Gillingham et al., 2004). If a similar function could be assumed in plants, the role of ARF1 in retrograde transport could potentially be related to its function in GDAP1 recruitment. In addition, GDAP1 has been identified as a member of the golgin family (Latijnhouwers et al., 2005) and some golgins have been linked to tethering events at the Golgi apparatus in mammalian cells (Short et al., 2005). It is therefore also possible that the subcellular distribution of GDAP1 may be linked to processes of tethering at the Golgi apparatus and with extra-Golgi structures to facilitate vesicle transport for post-Golgi traffic.

The Recruitment of Multiple ARF1 Effectors on Different Membranes Implies That the Membrane Environment Influences the Role of the GTPase

The observation that the subcellular distributions of GDAP1 and COPI overlap only partially raises the question of how GDAP1 and other ARF1 effectors are recruited to a specific membrane containing active ARF1. The codistribution of ARF1 with COPI and GDAP1 on the Golgi and the exclusive colocalization of the GTPase with GDAP1 on the extra-Golgi structures imply that the recognition of effectors by ARF1 occurs in conjunction with determinants for a specific spatial distribution. One possibility is that at least two different receptors of ARF1 may exist separately on Golgi and extra-Golgi membranes. This model, however, would not be sufficient to explain how COPI and GDAP1 achieve partial colocalization. Another hypothesis to explain the differential distribution of COPI and GDAP1 is linked to the cellular role of these effectors. Retrograde COPI cargo is recycled to the ER from the cis-Golgi where coatomer preferentially resides (Storrie et al., 2000; Ritzenthaler et al., 2002). It is possible that recognition of specific signals on retrograde COPI cargo molecules, such as the dilysine motif (Contreras et al., 2004) as well as active ARF1, is necessary for coatomer to be engaged at Golgi membranes. At the same time, a cytosolic COPI pool may also target the non-Golgi structures via ARF1 recruitment; however, COPI would not be engaged there, because the COPI cargo with signals for COPI recruitment are not present on these membranes due to efficient COPI cargo recycling from the Golgi to the ER. On the contrary, recruitment of GDAP1 on the Golgi and extra-Golgi membranes may not require a mechanism similar to COPI to reside on membranes and its recruitment may be linked exclusively to the distribution of ARF1. Our findings that GDAP1 cycles with kinetics that tightly overlap those of ARF1 (Fig. 5) support this view. This model suggests that ARF1 works as a molecular switch for the recruitment and activation of ARF1-selected effectors. From this perspective, the specific functions of ARF1 would be achieved by the biological role of ARF1 effectors and their membrane environment.

The Effectors of ARF1 Have Different Kinetics on Membranes

By comparing the kinetics of ARF1, COPI, and GDAP1 on membranes by FRAP analyses, we have determined that GDAP1 and ARF1 cycle on and off membranes at a similar rate that is faster than coatomer (Fig. 5). Different kinetics of ARF1 and COPI have been shown in both mammalian and plant cells, and it was suggested that the faster dissociation of ARF1 from membranes in comparison to coatomer

could serve to establish a COPI domain on the Golgi apparatus (Presley et al., 2002; Stefano et al., 2006a). Taken together, our data suggest that the dynamics of the COPI coat and GDAP1 are linked to the activation of ARF1 but that they are not linked to each other, and that GDAP1 may not be involved directly in the dynamic formation of the COPI domain at the Golgi membranes. This does not exclude the possibility that GDAP1 may be involved in events downstream of COPI vesicle budding.

In cells treated with BFA, it has been shown that COPI coat is released from the Golgi membranes prior to ARF1, while the Golgi cisternae, including the cis-Golgi, remain intact (Ritzenthaler et al., 2002). Our data are consistent with these findings and they show not only that GDAP1 remains bound to membranes longer than εCOP in response to BFA (Fig. 7) but also that ARF1 and GDAP1 cycle at the same rate (Fig. 5). These data may be explained by considering the involvement of COPI coat in selection of retrograde cargo. BFA affects ER export to the extent that Golgi membranes collapse into the ER (Ritzenthaler et al., 2002; Saint-Jore et al., 2002), ER export site integrity is lost (daSilva et al., 2004; Stefano et al., 2006a), and ER to Golgi transport is restricted (Brandizzi et al., 2002). Therefore, a depletion of COPI cargo in the Golgi coupled with ARF1 inactivation upon BFA treatment may inhibit COPI recruitment on the Golgi due to depletion of COPI cargo signals.

In conclusion, our data support an additional function of ARF1 in plants and suggest a new level of control for ARF1 activity that is linked to the spatial distribution of the GTPase. The plant Golgi apparatus is a highly dynamic organelle and numerous proteins are involved in the structural organization essential for its function. ARF1 carries out an important regulatory role and an appreciation for the control of this and other GTPases will be key to understanding how these molecules and their effectors are organized in time and space. Future work will likely be aimed at understanding both the function of golgins in plant cells and identifying the specific ARF-guanine exchange factors responsible for activation of ARF1 at various locations.

MATERIALS AND METHODS

Molecular Cloning

Standard molecular techniques were used for subcloning. The fluorescent proteins used in this study were based on fluorescent fusions with mGFP5 (Haseloff et al., 1997), ECFP, or EYFP (CLONTECH). The spectral properties of mGFP5 allow efficient spectral separation from YFP (Brandizzi et al., 2002). ERD2 was used as a Golgi marker (Lee et al., 1993) fused to GFP (Boevink et al., 1998). cDNA of GDAP1 (At3g61570) was obtained as an Arabidopsis Biological Resource Center clone and amplified by PCR primers containing the *Xba*I and *Bam*HI sites for subcloning downstream of either YFP or CFP in the binary vector pVKH18-En6. For coatomer labeling, we used a YFP fusion with the Arabidopsis (*Arabidopsis thaliana*) homolog of εCOP, a component of the COPI coatomer (Stefano et al., 2006a). For expression based on stable DNA integration of untagged Arabidopsis ARF1 in its GTP-restricted form (Pimpl et al., 2003) mediated by Agrobacterium, we used a modified binary vector pVKH18-En6 bearing two 35S-pNOS reading cassettes in direct orientation, as previously described (Stefano et al., 2006a). For His_6 and GST-tagged proteins, DNA sequences of GDAP1 and wild-type and mutant ARF1 proteins (Q71L [GTP] and T31N [GDP]) were subcloned in recombinant *Escherichia coli* expression vectors pET-28b(+) (Novagen) or in pGEX (Amersham), respectively. The His_6-tag was placed downstream of the ARF1 sequence and the GST tag was upstream of the GDAP1 sequence. The primer sequences used for the subcloning indicated above are available upon request.

Sampling, Imaging, and Spot FRAP

Transformed leaves were analyzed 44 to 48 h after infection of the lower epidermis. Confocal imaging was performed using an upright LSM Zeiss 510 META, and either a 40× or 63× water immersion objective. For imaging expression of GFP constructs, YFP constructs, or both, imaging settings were used as described in Brandizzi et al. (2002) with a 1- to 3-μm optical slice. For simultaneous imaging of the triple labeling (FM4-64, YFP, and GFP), the fluorescence of FM4-64, ST-YFP, and ARF1-GFP was detected using the 594-, 514-, and 405-nm laser lines of HeNe, Argon, and blue diode lasers, respectively. The imaging configuration of the microscope was set with a main dichroic HFT 405/514/594, and emission filters 530 to 600 and 475 to 525 nm (for YFP and GFP, respectively) and 636 to 743 spectral dye separation settings of the LSM 510 META (for FM4-64). Simultaneous imaging was carried out using the line-sequential multitrack scanning mode configuration of the microscope.

Time-lapse scanning was acquired with imaging system software of the microscope.

Spot FRAP experiments for fluorochrome photobleaching and half-time computation were performed as described by Brandizzi et al. (2002). Segments of transformed leaves (approximately 5 mm^2) were submerged in 25 μM latrunculin B (Calbiochem; stock solution, 10 mM in dimethyl sulfoxide) for 1 h prior to photobleaching experiments to prevent movement of Golgi bodies and additional non-Golgi structures (Brandizzi et al., 2002; Stefano et al., 2006a). Significance was determined using a Student's two-tailed *t* test for two samples, assuming equal variance.

For experiments investigating the effects of BFA, segments of tissue were pretreated for 45 min with latrunculin B to stop Golgi movement, as described above. To follow the effects of BFA, we subsequently immersed leaf segments in a solution containing 25 μM latrunculin B and 100 μg/mL BFA and directly mounted the leaf segment on a slide in the latrunculin B/BFA solution. For control time-lapse experiments, segments of tissue were mounted in latrunculin B alone. When drugs were not used, leaf tissue was mounted on a slide in water alone.

Quantification of relative punctate structure fluorescence (RPSF) for GDAP1 and εCOP with and without $ARF1^{Q71L}$ was calculated by measuring the fluorescence intensity values (arbitrary units) using ImageJ software: (1) in a circle of 25-pixel diameter centered on a punctate structure; and (2) in a circle of the same dimensions adjacent to the punctate structure, covering a region containing cytosol (C). RPSF was then calculated as a percentage of the total fluorescence of both areas: $RPSF = (PS/[PS + C]) \times 100$. Measurements were performed on images acquired with the same microscope settings of laser intensity, detector gain, offset, and maximum pinhole aperture. Postacquisition image processing was done with a Corel Draw 12 imaging suite.

We followed the relative Golgi fluorescence for εCOP-YFP and YFP-GDAP1 with and without ARF1-GFP (±BFA treatment), as well as coexpression of εCOP-YFP and CFP-GDAP1 (±BFA treatment), by measuring the fluorescence intensity values over time as described above on each frame of the time lapse over 10 min. The RPSF was then calculated as a percentage of the total fluorescence for each punctate structure. Fluorescence data were graphed with respect to time and trend lines were applied by calculating a polynomial curve fit.

FM4-64 Labeling

Leaves were infiltrated through the stomata on the abaxial surface with a solution of FM4-64 (Molecular Probes) at a concentration of 8.2 μM in water. Samples of leaf tissue were excised from the leaves 5 to 10 min after infiltration, mounted in the FM4-64 solution on a slide, and observed up to 1 h postinfiltration.

In Vivo and in Vitro Expression

Four-week-old tobacco (*Nicotiana tabacum*) cv Petit Havana greenhouse plants grown at 25°C were used for imaging experiments (Batoko et al., 2000).

For in vitro experiments, protein production of His_6 and GST fusions subcloned in pET-28b(+) and pGEX vectors was induced in *E. coli* BL21(DE3) cells as previously described (Stefano et al., 2006b). Cultures were grown to an OD_{600} of 1.0, and protein production was induced with the addition of 1 mm isopropylthio-β-galactoside and further incubated for 5 h at 30°C. Cells were then pelleted and lysed according to the instructions provided by the manufacturer of the glutathione resin columns (BD Biosciences) for binding GST-tagged proteins. In both cases, *E. coli* extracts were prepared under native conditions to discharge insoluble proteins in the pellet; they were cleared of inclusion bodies by centrifugation (12,000*g* for 30 min). The supernatant was used for further analyses. For protein-protein interaction assays, the GST extracts were loaded into glutathione resin columns (BD Biosciences) for binding of GST-tagged proteins. Protein binding, removal of endogenous proteins, and elution of tagged proteins were performed according to the manufacturer's instructions.

Glutathione-Agarose Affinity Chromatography

To ensure that equal amounts of GST and GST-GDAP1 were mixed with His_6-tagged ARF1 protein extracts, 500 mL of overnight *E. coli* culture expressing GST-GDAP1 was extracted in 10 mL of GST extraction buffer (BD Biosciences) and mixed with 500 μL of agarose beads. The bead slurry was divided into 150-μL aliquots and incubated with recombinant His_6-tagged wild-type ARF1, $ARF1^{Q71L}$, $ARF1^{T31N}$, or ARF1 incubated with either 100 μM GTPγS (Sigma) or 100 μM GDPβS (Sigma), or His_6 protein at 4°C for 3 h with gentle rotation. The beads were centrifuged at 4°C, 500*g*, for 1 min and then washed three times with nucleotide stabilization buffer (20 mm HEPES, pH 7.5, 100 mm NaCl, 5 mm $MgCl_2$). Bound proteins were eluted from the beads with an appropriate volume of 5× SDS-PAGE sample buffer (0.225 M Tris-HCl, pH 6.8; 50% glycerol; 5% SDS; 0.05% bromphenol blue; 5% β-mercaptoethanol), boiled for 5 min, and equal volumes were run on a 12% SDS-PAGE gel. Protein was transferred to a nitrocellulose membrane by electroblotting and blocked with phosphate-buffered saline plus 0.05% Tween 20 and 5% milk powder for 2 h. The nitrocellulose was then incubated in phosphate-buffered saline plus Tween 20 containing 1% milk powder and either anti-GST serum from rabbit (AbCam) at a dilution of 1:500 or anti-His_6 serum from rabbit (Santa-Cruz Biotechnology) at a dilution of 1:200 for 4 h. A horseradish peroxidase-conjugated anti-rabbit IgG (Sigma) was subsequently used to detect the protein of interest and an enhanced chemiluminescence substrate (Millipore) was used to detect the signal. We acquired a chemiluminescence signal using an Epichem3 Darkroom gel documentation system (UVP BioImaging Systems) with Labworks Image Acquisition software without digital enhancement. Biochemical results presented in this article are representative of at least three independent repetitions.

Sequence data from this article can be found in the GenBank/EMBL data libraries under accession number GI:42566118 (At3g61570).

Supplemental Data

The following materials are available in the online version of this article.

Supplemental Figure S1. The non-Golgi structure labeled by ARF1 partially overlaps with FM4-64.

Supplemental Figure S2. YFP-GDAP1 and ARF1-GFP maintain fluorescence without BFA treatment.

Supplemental Figure S3. εCOP-YFP and ARF1-GFP maintain fluorescence without BFA treatment.

Supplemental Figure S4. εCOP-YFP and CFP-GDAP1 maintain fluorescence without BFA treatment.

Received December 18, 2006; accepted February 7, 2007; published February 16, 2007.

LITERATURE CITED

Batoko H, Zheng HQ, Hawes C, Moore I (2000) A rab1 GTPase is required for transport between the endoplasmic reticulum and Golgi apparatus and for normal Golgi movement in plants. Plant Cell **12:** 2201–2218

Boevink P, Oparka K, Santa Cruz S, Martin B, Betteridge A, Hawes C (1998) Stacks on tracks: the plant Golgi apparatus traffics on an actin/ER network. Plant J **15:** 441–447

Bolte S, Talbot C, Boutte Y, Catrice O, Read ND, Satiat-Jeunemaitre B (2004) FM-dyes as experimental probes for dissecting vesicle trafficking in living plant cells. J Microsc **214:** 159–173

Brandizzi F, Snapp EL, Roberts AG, Lippincott-Schwartz J, Hawes C (2002) Membrane protein transport between the endoplasmic reticulum and the Golgi in tobacco leaves is energy dependent but cytoskeleton independent: evidence from selective photobleaching. Plant Cell **14:** 1293–1309

Contreras I, Ortiz-Zapater E, Aniento F (2004) Sorting signals in the cytosolic tail of membrane proteins involved in the interaction with plant ARF1 and coatomer. Plant J **38:** 685–698

Contreras I, Ortiz-Zapater E, Castilho LM, Aniento F (2000) Characterization of Cop I coat proteins in plant cells. Biochem Biophys Res Commun **273:** 176–182

Couchy I, Bolte S, Crosnier MT, Brown S, Satiat-Jeunemaitre B (2003) Identification and localization of a beta-COP-like protein involved in the morphodynamics of the plant Golgi apparatus. J Exp Bot **54:** 2053–2063

daSilva LL, Snapp EL, Denecke J, Lippincott-Schwartz J, Hawes C, Brandizzi F (2004) Endoplasmic reticulum export sites and Golgi bodies behave as single mobile secretory units in plant cells. Plant Cell **16:** 1753–1771

Dettmer J, Hong-Hermesdorf A, Stierhof YD, Schumacher K (2006) Vacuolar H+-ATPase activity is required for endocytic and secretory trafficking in Arabidopsis. Plant Cell **18:** 715–730

Donaldson JG, Cassel D, Kahn RA, Klausner RD (1992) ADP-ribosylation factor, a small GTP-binding protein, is required for binding of the coatomer protein beta-COP to Golgi membranes. Proc Natl Acad Sci USA **89:** 6408–6412

Donaldson JG, Honda A, Weigert R (2005) Multiple activities for Arf1 at the Golgi complex. Biochim Biophys Acta **1744:** 364–373

Faure J, Stalder R, Borel C, Sobo K, Piguet V, Demaurex N, Gruenberg J, Trono D (2004) ARF1 regulates Nef-induced CD4 degradation. Curr Biol **14:** 1056–1064

Gaynor EC, Chen CY, Emr SD, Graham TR (1998) ARF is required for maintenance of yeast Golgi and endosome structure and function. Mol Biol Cell **9:** 653–670

Gillingham AK, Tong AH, Boone C, Munro S (2004) The GTPase Arf1p and the ER to Golgi cargo receptor Erv14p cooperate to recruit the golgin Rud3p to the cis-Golgi. J Cell Biol **167:** 281–292

Gu F, Gruenberg J (2000) ARF1 regulates pH-dependent COP functions in the early endocytic pathway. J Biol Chem **275:** 8154–8160

Haseloff J, Siemering KR, Prasher DC, Hodge S (1997) Removal of a cryptic intron and subcellular localization of green fluorescent protein are required to mark transgenic Arabidopsis plants brightly. Proc Natl Acad Sci USA **94:** 2122–2127

Lam SK, Siu CL, Hillmer S, Jang S, An G, Robinson DG, Jiang L (2007) Rice SCAMP1 defines clathrin-coated, trans-Golgi-located tubular-vesicular structures as an early endosome in tobacco BY-2 cells. Plant Cell **19:** 296–319

Latijnhouwers M, Hawes C, Carvalho C (2005) Holding it all together? Candidate proteins for the plant Golgi matrix. Curr Opin Plant Biol **8:** 632–639

Lee HI, Gal S, Newman TC, Raikhel NV (1993) The Arabidopsis endoplasmic reticulum retention receptor functions in yeast. Proc Natl Acad Sci USA **90:** 11433–11437

Memon AR (2004) The role of ADP-ribosylation factor and SAR1 in vesicular trafficking in plants. Biochim Biophys Acta **1664:** 9–30

Movafeghi A, Happel N, Pimpl P, Tai GH, Robinson DG (1999) Arabidopsis Sec21p and Sec23p homologs: probable coat proteins of plant COP-coated vesicles. Plant Physiol **119:** 1437–1446

Nebenführ A, Ritzenthaler C, Robinson DG (2002) Brefeldin A: deciphering an enigmatic inhibitor of secretion. Plant Physiol **130:** 1102–1108

Pimpl P, Hanton SL, Taylor JP, Pinto-DaSilva LL, Denecke J (2003) The GTPase ARF1p controls the sequence-specific vacuolar sorting route to the lytic vacuole. Plant Cell **15:** 1242–1256

Pimpl P, Movafeghi A, Coughlan S, Denecke J, Hillmer S, Robinson DG (2000) In situ localization and in vitro induction of plant COPI-coated vesicles. Plant Cell **12:** 2219–2236

Presley JF, Ward TH, Pfeifer AC, Siggia ED, Phair RD, Lippincott-Schwartz J (2002) Dissection of COPI and Arf1 dynamics in vivo and role in Golgi membrane transport. Nature **417:** 187–193

Price HP, Stark M, Smith DF (2007) Trypanosoma brucei ARF1 plays a central role in endocytosis and Golgi-lysosome trafficking. Mol Biol Cell **18:** 864–873

Puertollano R, Randazzo PA, Presley JF, Hartnell LM, Bonifacino JS (2001) The GGAs promote ARF-dependent recruitment of clathrin to the TGN. Cell **105:** 93–102

Ritzenthaler C, Nebenführ A, Movafeghi A, Stussi-Garaud C, Behnia L, Pimpl P, Staehelin LA, Robinson DG (2002) Reevaluation of the effects of brefeldin A on plant cells using tobacco Bright Yellow 2 cells expressing Golgi-targeted green fluorescent protein and COPI antisera. Plant Cell **14:** 237–261

Robineau S, Chabre M, Antonny B (2000) Binding site of brefeldin A at the interface between the small G protein ADP-ribosylation factor 1 (ARF1) and the nucleotide-exchange factor Sec7 domain. Proc Natl Acad Sci USA **97:** 9913–9918

Saint-Jore CM, Evins J, Batoko H, Brandizzi F, Moore I, Hawes C (2002) Redistribution of membrane proteins between the Golgi apparatus and endoplasmic reticulum in plants is reversible and not dependent on cytoskeletal networks. Plant J **29:** 661–678

Serafini T, Orci L, Amherdt M, Brunner M, Kahn RA, Rothman JE (1991) ADP-ribosylation factor is a subunit of the coat of Golgi-derived COP-coated vesicles: a novel role for a GTP-binding protein. Cell **67:** 239–253

Short B, Haas A, Barr FA (2005) Golgins and GTPases, giving identity and structure to the Golgi apparatus. Biochim Biophys Acta **1744:** 383–395

Stamnes MA, Rothman JE (1993) The binding of AP-1 clathrin adaptor particles to Golgi membranes requires ADP-ribosylation factor, a small GTP-binding protein. Cell **73:** 999–1005

Stefano G, Renna L, Chatre L, Hanton SL, Moreau P, Hawes C, Brandizzi F (2006a) In tobacco leaf epidermal cells, the integrity of protein export from the endoplasmic reticulum and of ER export sites depends on active COPI machinery. Plant J **46:** 95–110

Stefano G, Renna L, Hanton SL, Chatre L, Haas TA, Brandizzi F (2006b) ARL1 plays a role in the binding of the GRIP domain of a peripheral matrix protein to the Golgi apparatus in plant cells. Plant Mol Biol **61:** 431–449

Storrie B, Pepperkok R, Nilsson T (2000) Breaking the COPI monopoly on Golgi recycling. Trends Cell Biol **10:** 385–391

Takeuchi M, Ueda T, Yahara N, Nakano A (2002) Arf1 GTPase plays roles in the protein traffic between the endoplasmic reticulum and the Golgi apparatus in tobacco and Arabidopsis cultured cells. Plant J **31:** 499–515

Teal SB, Hsu VW, Peters PJ, Klausner RD, Donaldson JG (1994) An activating mutation in ARF1 stabilizes coatomer binding to Golgi membranes. J Biol Chem **269:** 3135–3138

Xu J, Scheres B (2005) Dissection of Arabidopsis ADP-RIBOSYLATION FACTOR 1 function in epidermal cell polarity. Plant Cell **17:** 525–536

Yahara N, Ueda T, Sato K, Nakano A (2001) Multiple roles of Arf1 GTPase in the yeast exocytic and endocytic pathways. Mol Biol Cell **12:** 221–238

Zhang CJ, Rosenwald AG, Willingham MC, Skuntz S, Clark J, Kahn RA (1994) Expression of a dominant allele of human ARF1 inhibits membrane traffic in vivo. J Cell Biol **124:** 289–300